Inorganic Chemistry

Article

pubs.acs.org/IC

A Heteroleptic Bis(tridentate) Ruthenium(II) Platform Featuring an Anionic 1,2,3-Triazolate-Based Ligand for Application in the Dye-Sensitized Solar Cell

Stephan Sinn,[†,‡,△] Benjamin Schulze,[†,‡,△] Christian Friebe,[†,‡] Douglas G. Brown,[§] Michael Jäger,[†,‡] Joachim Kübel,[⊥,▽] Benjamin Dietzek,[⊥,▽,‡,*] Curtis P. Berlinguette,[§,∥,*] and Ulrich S. Schubert[†,‡,*]

[†]Laboratory of Organic and Macromolecular Chemistry (IOMC), Friedrich Schiller University Jena, Humboldtstr. 10, 07743 Jena, Germany

[‡]Jena Center for Soft Matter (JCSM), Friedrich Schiller University Jena, Philosophenweg 7, 07743 Jena, Germany

[§]Department of Chemistry, University of Calgary, 2500 University Drive N.W., Calgary, Alberta, Canada T2N 1N4

[∥]Department of Chemistry, The University of British Columbia, 2036 Main Mall, Vancouver, British Columbia, Canada V6T 1Z1

[⊥]Institute of Physical Chemistry (IPC) and Abbe Center of Photonics, Friedrich Schiller University Jena, Helmholtzweg 4, 07743 Jena, Germany

[▽]Leibniz Institute of Photonic Technology (IPHT), Albert-Einstein-Str. 9, 07745 Jena, Germany

Supporting Information

ABSTRACT: A series of bis(tridentate) ruthenium(II) complexes featuring new anionic 1,2,3-triazolate-based tridentate ligands and 2,2′:6′,2″-terpyridine is presented. For a complex equipped with carboxy anchoring groups, the performance in a dye-sensitized solar cell is evaluated. The title complexes are readily synthesized and can be decorated with alkyl chains utilizing azide−alkyne cycloaddition methods, in order to improve the device stability and allow the use of alternative electrolytes. On account of the strong electron donation from the 1,2,3-triazolates, the complexes exhibit a broad metal-to-ligand charge-transfer absorption (up to 700 nm), leading to an electron transfer toward the anchoring ligand. The lifetimes of the charge-separated excited states are in the range of 50 to 80 ns. In addition, the ground- and excited-state redox potentials are appropriate for the application in dye-sensitized solar cells, as demonstrated by power conversion efficiencies of up to 4.9% (vs 6.1% for **N749**).

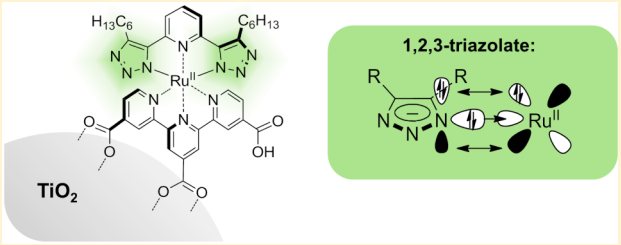

INTRODUCTION

Dye-sensitized solar cells (DSSCs) rely on the sensitization of a wide-band-gap semiconductor such as TiO_2 with dye molecules. The sensitizer needs to be photo- and redox-stable, absorb as much light as possible, and feature excited- and ground-state redox potentials that allow for efficient electron injection into the conduction band of the semiconductor and subsequent regeneration by the electrolyte, respectively.[1,2] Meanwhile, power conversion efficiencies (PCEs) of up to 12.3% have been achieved with molecular dyes[3] and ruthenium(II) polypyridyl complexes featuring thiocyanato ligands, such as $(NBu_4)_3[Ru(Htctpy)(NCS)_3]$ (**N749** or black dye; Htctpy = 2,2′:6′,2″-terpyridine-4′-carboxylic acid-4,4″-dicarboxylate) (Figure 1), are among the most efficient sensitizers, with PCEs up to 11.4%.[4−7] However, the monodentate thiocyanato ligands preclude further optimization *via* ligand functionalization and limit the lifetime of DSSCs, as they can decoordinate easily.[8,9] Consequently, the thiocyanate ligands have been replaced by anionic multidentate ligands including anionic phenyl rings,[10−16] tetrazolates,[17] 1,2,4-triazolates,[18−20] and pyrazolates,[20−23] enabling an improved long-term stability and similar or higher PCEs compared to thiocyanate-based benchmark dyes.[24] Moreover, these chelating ligands enable the introduction of hydrophobic alkyl chains and additional chromophores to further improve the DSSC life span[18,25−27] and the light-harvesting capability, respectively.[24]

Chou and co-workers presented ruthenium(II) dyes featuring functionalized dianionic 2,6-bis(5-pyrazolyl)pyridine ligands (Figure 1), which achieved remarkable PCEs of 9.1% (TF-1) and 10.7% (TF-2, vs 9.2% for **N749**) in the DSSC.[23] Building on these promising results, we present herein a series of heteroleptic bis(tridentate) ruthenium(II) complexes containing anionic 1,2,3-triazolates as thiocyanate surrogates (Figure 1). This approach benefits from a very simple ligand synthesis *via* azide−alkyne cycloaddition, which also allows the ready installation of alkyl chains. In comparison to the parent, charge-neutral 1,2,3-triazoles,[28−30] the σ lone pair and the π system of anionic triazolates are raised in energy, resulting in an enhanced σ- and π-donor strength. Furthermore, the use of

Received: October 27, 2013
Published: January 21, 2014

   dx.doi.org/10.1021/ic402701v | *Inorg. Chem.* 2014, 53, 1637−1645

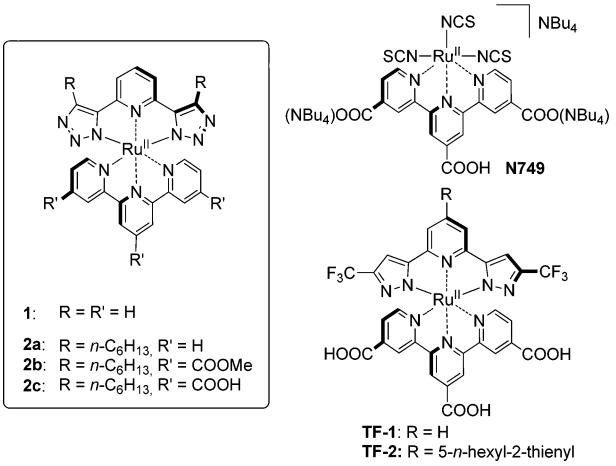

Figure 1. Schematic representation of the ruthenium(II) complexes **1** and **2a**–**2c** and related literature examples.[4,23]

1,2,3-triazolates circumvents the formation of coordination isomers, which plague analogous 1,2,4-triazolate-based ruthenium(II) complexes (Figure 2),[31] and, in contrast to related pyrazolate complexes,[23] no electron-withdrawing groups need to be installed to raise the Ru(III)/Ru(II) redox potential, due to the higher degree of *aza* substitution of the 1,2,3-triazolate.

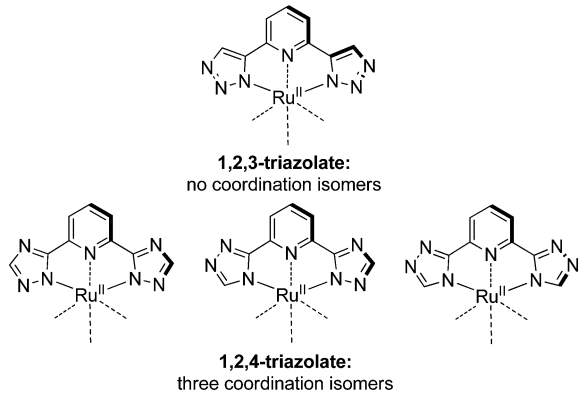

Figure 2. Schematic illustration of the formation of isomeric ruthenium(II) complexes with tridentate ligands based on 1,2,4-triazolates.

RESULTS AND DISCUSSION

Synthesis. The 2,6-bis(1,2,3-triazol-4-yl)pyridine ligands were synthesized either *via* Cu(I)-catalyzed azide–alkyne cycloaddition, using *in situ* generated hydroxymethyl azide,[32] followed by a base-induced cleavage of formaldehyde, or, in the case of the internal alkyne (see Scheme 1 and the Supporting Information (SI)), *via* a thermal azide–alkyne cycloaddition with azidomethyl pivalate.[33] For the latter, the cycloadduct is obtained as a statistically distributed mixture; however, after cleavage in basic media and subsequent reprotonation, the free NH-triazole is obtained, which undergoes rapid tautomerization.[30] The corresponding ruthenium(II) complexes were obtained in good yields utilizing $[Ru^{II}(tpy)(MeCN)_3](PF_6)_2$ (tpy = 2,2′:6′,2″-terpyridine) or $[Ru^{II}(tcmtpy)(MeCN)_3](PF_6)_2$ (tcmtpy = 4,4′,4″-tricarboxymethyl-2,2′:6′,2″-terpyridine; see Scheme 1 and the SI) as precursor.[34] The subsequent saponification of **2b** was achieved as described previously.[12]

Scheme 1. Schematic Representation of the Synthesis of Complexes 1 and 2a–2c, and the Numbering Scheme of the Studied Complexes[a]

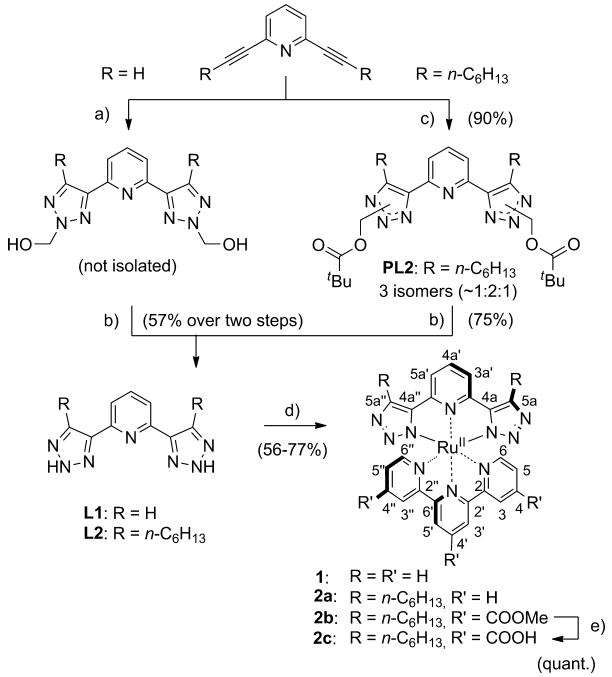

[a]Conditions: (a) $HCHO_{aq}$, AcOH, NaN_3, $CuSO_4$, sodium ascorbate, dioxane, rt, 24 h. (b) NaOH, $MeOH/H_2O$, rt, 24 h. (c) Azidomethyl pivalate, 100 °C, 72 h. (d) $[Ru^{II}(tpy)(MeCN)_3](PF_6)_2$ or $[Ru^{II}(tcmtpy)(MeCN)_3](PF_6)_2$, alcohol, or triethylene glycol dimethyl ether, 150 °C, 30 min, microwave irradiation. (e) $DMF/NEt_3/H_2O$ (3:1:1 *v*/*v*/*v*).

The solubilities of the charge-neutral complexes are expectedly low; however, the introduction of the alkyl chains (**2a**–**2c**) improves the solubility, allowing the investigation of the photophysical and electrochemical properties (*vide infra*).

Computational Methods. To enable a deeper understanding of the electronic properties of the new ruthenium(II) complexes, density functional theory (DFT) calculations have been performed for **2a**–**2c** (note that the hexyl chains have been replaced by methyl groups to shorten the computing time). Additionally, the electronic properties of the fully deprotonated form of **2c** (**2c**′) were calculated, while the electronic excitations for **2c** were computed with the help of time-dependent (TD) DFT.[23] The calculations revealed that the highest occupied molecular orbital (HOMO) of the complexes is composed of a metal d orbital and π orbitals located on the triazolate rings, which is expected in view of the electron-rich π system of the anionic ring.[18,22,24] As a result of the electron repulsion between the anionic ligand and the metal center, the HOMO is strongly destabilized in comparison to polypyridyl complexes such as $[Ru(tpy)_2](PF_6)_2$. For **2a**–**2c**, the lowest unoccupied molecular orbital (LUMO) is mainly composed of π^* orbitals of the terpyridine ligand (Table S2). Relative to **2a**, the HOMO and, in particular, the LUMO of **2b** are stabilized due to the electron-withdrawing −COOMe groups, resulting in a significantly smaller HOMO–LUMO gap. The −COOH anchoring groups of **2c** have a similar effect on the frontier orbitals energies. In contrast, when compared to **2a**, the HOMO and LUMO of the fully deprotonated complex **2c**′ are destabilized and the HOMO–LUMO gap is slightly larger

dx.doi.org/10.1021/ic402701v | *Inorg. Chem.* 2014, 53, 1637–1645

(Figure S11), which is attributed to the electron-donating effect of the $-COO^-$ groups. The most relevant electronic transitions of **2c** are displayed in Figure 3 along with the corresponding

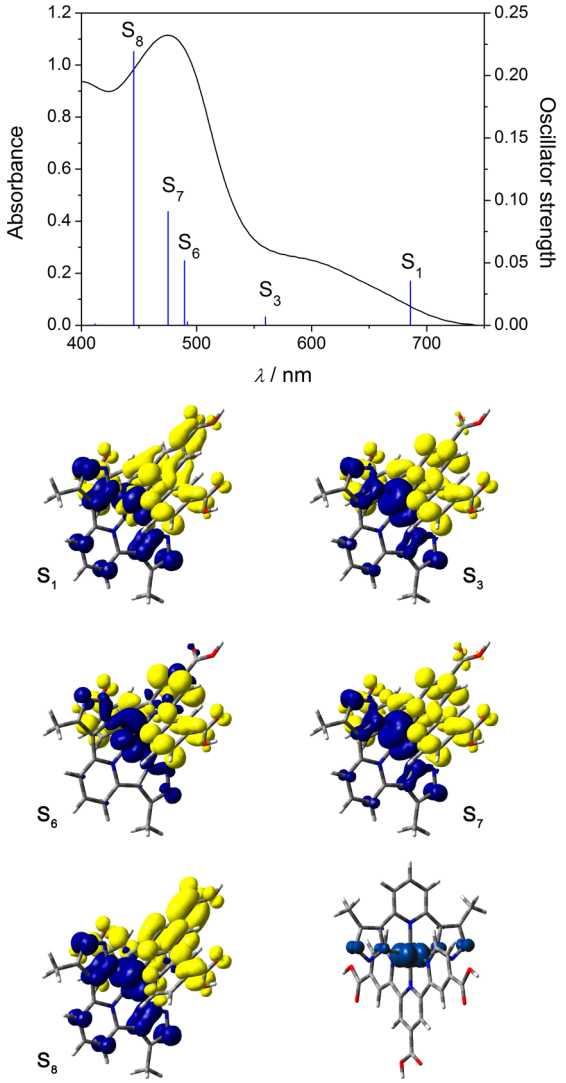

Figure 3. Top: Experimental UV–vis absorption spectrum of **2c** adsorbed on TiO_2 (12 μm thick, transparent film, active area of 0.88 cm^2) and calculated vertical singlet–singlet transitions of **2c**. Bottom: Corresponding EDDM plots (blue and yellow represent depletion and accumulation, respectively, of electron density upon electronic excitation, isovalue = 0.001) and spin-density plot of the oxidized ground state (bottom right, isovalue = 0.004) of **2c**. Color code: carbon, gray; hydrogen, white; oxygen, red; nitrogen, blue; ruthenium, cyan. Note that the tpy ligand is functionalized with carboxy groups, which are known to electronically resemble Ti(IV)-coordinated carboxylates.[35]

electron-density difference maps (EDDM). The computed electronic excitations are in good agreement with the experimental UV–vis absorption spectrum (*vide infra*). The lowest-energy absorption (population of S_1) is a pure HOMO–LUMO transition, which can thus be assigned to a metal-to-ligand charge transfer (MLCT) with some ligand-to-ligand charge-transfer (LLCT) character. Also the other electronic transitions in the visible-light region are of MLCT character with varying LLCT contribution (Figure 3, population of S_3, S_6, S_7, and S_8). As the electron transfer is directed toward the anchoring tctpy ligand in each case, **2c** features an excited-state electronic structure suitable for electron injection into TiO_2.[36] To allow the estimation of the "hole distribution" resulting after photo-oxidation, the spin-density distribution was calculated for the oxidized complex. As a result, the hole is shared by the metal and the anionic ligand, which is believed to facilitate the sensitizer regeneration.[37,38]

Photophysics and Electrochemistry. The photophysical and electrochemical properties of the complexes are in line with the computational results. The increased σ- and π-donor strength of the anionic 1,2,3-triazolates relative to the neutral 1,2,3-triazoles[31,34,39] causes a destabilization of the metal d orbitals, resulting in a cathodically shifted Ru(III)/Ru(II) redox couple as well as bathochromically shifted MLCT transitions (Table 1). Consequently, a weak, plateau-like absorption band that extends to very long wavelengths is observed (Figures 4 and 5), which is typical for bis(tridentate) ruthenium(II) complexes featuring azolate donors.[21,23,31,40]

As the 1,2,3-triazolate rings of the ruthenium(II) complexes feature additional nitrogen donors, the complexes can be protonated (Figure 4) with the properties of the resulting complexes reflecting those of analogous 1,2,3-triazole ruthenium(II) complexes.[34,39] The protonation was investigated in more detail by UV–vis acid–base titration of **1** (Figures S1–S3). Within the studied pH range from 0 to 12, only one spectral change around pH 4 to 5 occurs; no isosbestic points are present, which indicates that there are more than two species involved. The first and second protonation of the triazolate ligand of **1** occur most likely both within the narrow pH window of 4 to 5, and thus, only a single pK_a value of about 4.7 could be determined (Figures S1 and S2). Furthermore, a weak emission appears upon increasing the pH value, which can be attributed to an increased destabilization of the deactivating triplet metal-centered (^{3}MC) excited states relative to the ^{3}MLCT state.[31,40,41] Accordingly, the excited-state lifetimes of **2a** (54 ns, Table 1) and **2c** (83 ns) are significantly prolonged relative to those of the related $[Ru(tpy)_2](PF_6)_2$ complex (0.21 ns)[42] and sufficiently long (>10 ns) to enable efficient electron injection into TiO_2 given that injection occurs on the picosecond time scale.[43] Comparison with analogous heteroleptic bis(tridentate) ruthenium(II) complexes featuring 1,2,4-triazolates or tetrazolates shows that **1** is less basic than the 1,2,4-triazolate complex but more basic than the tetrazolate counterpart.[31] Apparently, the cumulative arrangement of the nitrogen atoms within the 1,2,3-triazolate lowers the base strength relative to the 1,2,4-triazolate.[44] The corresponding excited-state lifetimes are slightly prolonged with increasing azolate donor strength.[31] Furthermore, in view of the similar excited-state lifetimes that are observed with related tris(bidentate) ruthenium(II) complexes featuring imidazolates,[45] the excited-state decay of the deprotonated complexes appears to be governed by the energy-gap law.[46]

As mentioned above, the $-COOMe$ groups cause a LUMO stabilization and, by increasing the π acidity of the tpy ligand, also a minor stabilization of the HOMO of **2b**. In the case of **2c**, the tctpy ligand (tctpy = 2,2′:6′,2″-terpyridine-4,4′,4″-tricarboxylic acid) features three successive deprotonation steps with corresponding pK_a values of approximately 1.2, 3.1, and 5.5.[4,34] In view of the above-mentioned pK_a values for the first and second protonation steps of the triazolate ligand of **1** (about 4.7), complex **2c** is expected to form a zwitterion in solution with two protons of the three carboxylic acid groups

dx.doi.org/10.1021/ic402701v | Inorg. Chem. 2014, 53, 1637–1645

Table 1. Photophysical and Electrochemical Data of Selected Ruthenium(II) Complexes

complex	λ_{Abs}/nm (ε /10^3 M^{-1} cm^{-1})	λ_{Em} (λ_{Ex})/nm	Φ_{PL}/%[a]	τ/ns[b]	$E_{1/2,ox}$/V vs Fc^+/Fc (vs NHE)[c]	E_{S*}/V vs Fc^+/Fc (vs NHE)[d]	E_{0-0}/eV[e]
1[f]	661s (0.3), 600s (0.8), 482 (5.2), 370 (5.2), 316 (29.9)	705 (490)	0.55	*g*	*g*	*g*	1.85
2a[f]	662 (0.7), 608 (0.9), 487 (5.6), 389 (4.4), 319 (30.5)	719 (490)	0.35	54	0.20 (0.83)	−1.60 (−0.97)	1.80
2b[f]	742 (2.3), 673 (2.7), 507 (8.9), 448 (10.7), 397 (13.7), 323 (28.7)	*h*	*h*	*h*	0.46 (1.09)		
2c	651(1.2), 602(2.1), 479(11.0), 388 (10.9), 320 (40.9)[i,j]	698 (480)[i,j]		83[i,j]	0.23 (0.86)[k]	−1.63 (−1.00)	1.86[j]
N749	620(6.5), 585(6.0), 420(10.5), 329(18.5)[l]	820[l]		30[m]	0.16 (0.85)[l]	−1.40 (−0.71)	1.58

[a]Determined using $[Ru(dqp)_2](PF_6)_2$ (in MeOH/EtOH 1:4, Φ_{PL} = 2.0%)[48] as reference; solutions were purged with N_2. [b]Air-equilibrated solution. [c]Unless stated otherwise, redox half-wave potentials were determined by cyclic voltammetry using Bu_4NPF_6 as the supporting electrolyte and Fc^+/Fc as the internal standard; conversion to NHE scale by addition of 0.63 V[49] and 0.69 V[50] when the measurement was done in MeCN and DMF/MeOH (4:1 *v*/*v*), respectively. [d]Calculated using $E_{S*} = E_{1/2,ox} - E_{0-0}$.[2] [e]Determined at the intersection of the absorption and emission spectra with the latter being normalized with respect to the lowest-energy absorption. [f]Measured in MeCN containing 0.5 M NEt_3. [g]Not measured due to low solubility. [h]Not observed with the used instrumental setup. [i]Measured in MeOH containing 0.5 M NEt_3. [j]Fully deprotonated species, see text. [k]Determined by square-wave voltammetry with the complex-anchored TiO_2 anode as the working electrode immersed in MeCN containing 0.5 M pyridine and 0.1 M Bu_4NPF_6 as the supporting electrolyte. [l]Measured in DMF/MeOH (4:1 *v*/*v*). [m]Measured in EtOH, taken from ref 4.

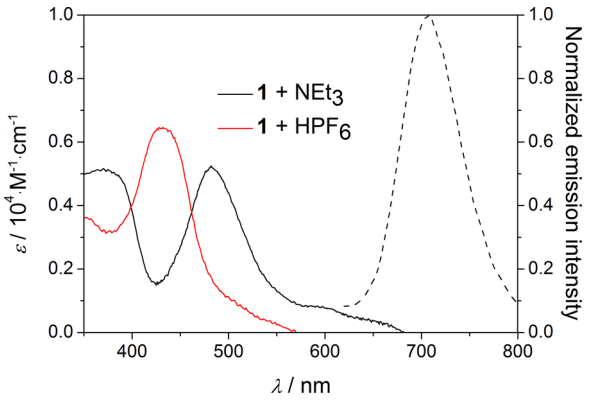

Figure 4. UV−vis absorption (solid) and room-temperature emission (dashed) spectra of **1** in the presence of NEt_3 and HPF_6 in MeCN.

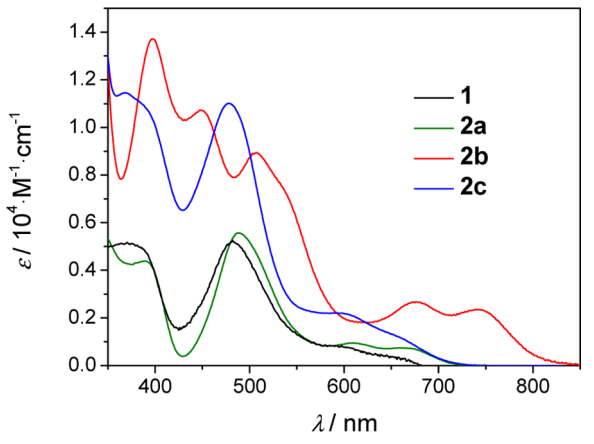

Figure 5. UV−vis absorption spectra of **1**, **2a**, **2b** (in MeCN + 0.5 M NEt_3), and **2c** (in MeOH + 0.5 M NEt_3).

being transferred to the triazolate rings. Thus, to provide a defined protonation state, the photophysical properties were determined in MeOH solution containing 0.5 M NEt_3 in order to ensure the complete deprotonation of the 1,2,3-triazolates. The UV−vis absorption and emission maxima are slightly hypsochromically shifted relative to **2a**, which is attributed to the LUMO destabilization by the three carboxylates. Notably, the E_{0-0} value determined for **2c** in solution (1.86 eV, Table 1) is therefore overestimated, which becomes obvious in view of the onset of the incident photon-to-current efficiency (IPCE) spectrum (*vide infra*), which occurs at 700 nm; that is, the E_{0-0} value for **2c** featuring TiO_2-coordinated carboxylates is at least 1.77 eV.

Importantly, due to the presence of 0.5 M 4-*tert*-butylpyridine (tBP) in the DSSC electrolyte (*vide infra*), the two triazolates of **2c** are deprotonated under working conditions. This assessment is corroborated by the measurement of the Ru(III)/Ru(II) redox potential of **2c** by square-wave voltammetry in acetonitrile containing 0.5 M pyridine with a **2c**-anchored TiO_2 anode as the working electrode. The measured value of 0.86 V vs NHE is between the redox potentials of **2a** and **2b** and considerably less positive than that for the analogous complex featuring charge-neutral 1,2,3-triazoles (1.61 V vs NHE),[34,39] which supports the presence of two anionic triazolates. Notably, the redox potential of **2c** is sufficiently high to ensure efficient regeneration by the relevant $I_2^{\bullet-}/I^-$ redox couple (0.79 V vs NHE).[47] Despite the above-mentioned difficulties to accurately determine the E_{0-0} value, a lower limit of the excited-state redox potential of **2c** can be determined from the ground-state redox potential and the minimum E_{0-0} value, which corresponds to the onset in the IPCE spectrum (750 nm or 1.65 eV). On this basis, the excited-state redox potential is at least −0.79 V vs NHE, which is sufficiently more negative than the conduction band edge of TiO_2 (ca. −0.7 V vs NHE)[43] and should enable efficient electron injection into the semiconductor.

Dye-Sensitized Solar Cells. To investigate the performance of **2c** in the DSSC, commercially available test cells were assembled according to literature procedures (*vide infra*)[51] and an electrolyte composition typically used for **N749** was chosen.[5] The obtained parameters are reported in Table 2. Under identical conditions, the PCEs of **2c** and **N749** are 4.0% and 6.1%, respectively. The lower V_{OC} and J_{SC} achieved with **2c** (Figure 6) were expected in view of the higher degree of protonation, which lowers the TiO_2 conduction-band energy,[35] and the lower light-harvesting capability. However, the IPCE spectrum not only reflects the inferior light harvesting at longer wavelengths but also reveals a lower IPCE maximum (Figure 7). When coadsorbed with chenodeoxycholic acid (cheno), **2c** allows a slightly higher V_{OC} and a significantly improved J_{SC}, in line with much higher IPCE values, resulting in a promising PCE of 4.9%. The significant enhancement of the photocurrent in the presence of cheno suggests that the relatively low IPCE

dx.doi.org/10.1021/ic402701v | *Inorg. Chem.* 2014, 53, 1637−1645

Table 2. Selected DSSC Data for the Ruthenium(II) Complexes Measured under AM1.5 Light Conditions[a]

dye	cheno	V_{oc}/V	J_{sc}/ mA cm^{-2}	FF	PCE/%
2c	no	0.61	8.9	0.70	4.0
2c	yes	0.62	11.8	0.63	4.9
N749	no	0.69	12.7	0.66	6.1

[a]Conditions: TiO_2 layer thickness of 12 μm (20 nm particles) + 3 μm (400 nm particles), active area of 0.28 cm^2; acetonitrile-based electrolyte containing 0.6 M 1,3-dimethylimidazolium iodide, 0.06 M I_2, 0.1 M LiI, 0.5 M tBP, and 0.1 M guanidinium thiocyanate.

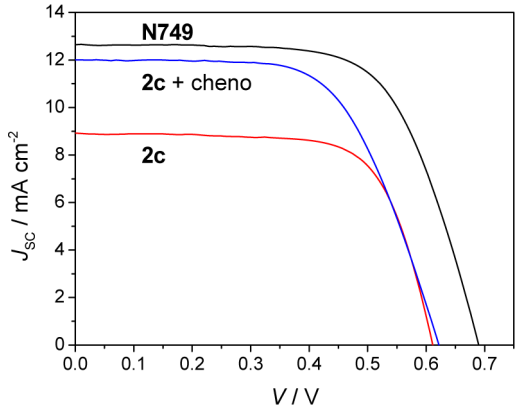

Figure 6. Selected $J-V$ curves of **2c** and **N749** (see Table 2 for conditions).

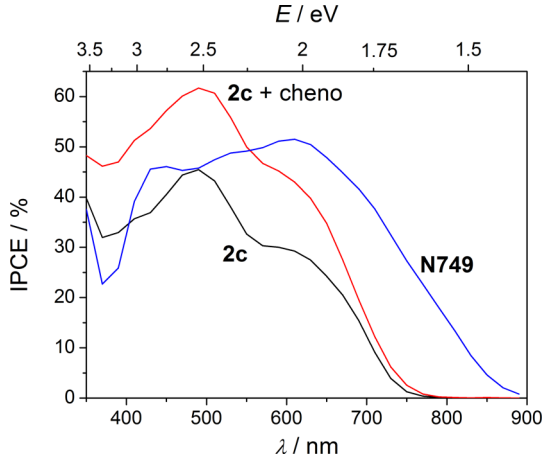

Figure 7. Photocurrent action spectra of **2c** and **N749**.

values observed in the absence of cheno are not caused by inefficient regeneration or injection but rather by more pronounced recombination reactions (*vide infra*). Similarly, it was reported that the PCE achieved with **N749** could be increased from 4.3 to 4.7% by coadsorption with cheno, although the higher PCE is mostly a result of an increased voltage.[52]

To better understand the effect of cheno, electrochemical impedance spectroscopy was performed (Figure S8).[16,51,53−56] A secondary effect is the lowering of the transport resistance (R_t), which is usually caused by a lowered TiO_2 conduction-band energy.[53] This effect may be ascribed to a reduced accessibility of the TiO_2 surface for the tBP electrolyte additive,[16] which is known to raise the conduction band.[57] The expected concomitant lowering of the recombination or charge-transfer resistance (R_{ct}) is apparently overcompensated by the lowered recombination tendency (*cf.* Table 2) as the TiO_2 surface passivation is improved by cheno. Accordingly, the V_{oc} is slightly enhanced by cheno. As a further result of the lowered R_t and the increased R_{ct}, the injected electrons can be collected much more efficiently, which is reflected by a normalized diffusion length well above 1[53] if **2c** is coadsorbed with cheno (Figure S8), which is in line with a higher J_{sc}. Without cheno, **N749** allows a higher R_{ct} than **2c**, which leads to an intermediate normalized diffusion length when compared to **2c** with and without cheno (Figure S8). The slightly higher recombination tendency for the sensitizer **2c** suggests a less effective surface coverage than for **N749** and/or interactions between iodine and **2c**. Nonetheless, **2c** is not expected to leave larger voids on the TiO_2 surface, since, even in the absence of cheno, a promising performance (J_{sc} = 6.2 mA cm^{-2}, V_{oc} = 0.70 V, FF = 0.58, PCE = 2.7%) was achieved in an initial attempt using a $[Co^{III}(bpy)_3](PF_6)_3/[Co^{II}(bpy)_3](PF_6)_2$-containing electrolyte[14,58] (see SI). This is attributed to the decoration of **2c** with hexyl chains allowing a more effective protection of the TiO_2 surface from the bulky redox mediator and, thus, a diminution of recombination reactions, which are typically observed when using thiocyanate-based benchmark dyes and the same Co(III)/Co(II)-based redox shuttle.[14,59]

CONCLUSION

The new heteroleptic bis(tridentate) ruthenium(II) complex featuring 1,2,3-triazolates was accessed by a facile and modular synthesis and possesses photophysical and electrochemical properties suitable for DSSC application. In comparison to ruthenium(II) polypyridyl complexes ($[Ru(tpy)_2](PF_6)_2$), the presented compounds exhibit prolonged excited-state lifetimes and room-temperature emission. A promising DSSC performance was achieved with different types of electrolytes. Prospectively, the thiocyanate-free, bis(tridenate) sensitizer platform should enable an extended DSSC life span[18] and offers the potential to optimize the light-harvesting capability *via* attachment of additional chromophores at the central pyridine ring of the anionic ligand.[12,23]

EXPERIMENTAL SECTION

$[Ru^{II}(tpy)(MeCN)_3](PF_6)_2$,[34] $[Ru^{II}(tcmtpy)(MeCN)_3](PF_6)_2$,[34] 2,6-diethynylpyridine,[60] and azidomethyl pivalate[33] were synthesized according to literature procedures. Dry toluene was obtained from a Pure Solv MD-4-EN solvent purification system (Innovative Technologies Inc.). Triethylamine was dried over KOH. Methanol was dried by distillation over magnesium and kept under nitrogen using standard Schlenk techniques. Tcmtpy was purchased from hetcat. $[Ru(Htctpy)(NCS)_3](NBu_4)_3$ was purchased from Solaronix. All other chemicals were purchased from commercial suppliers and used as received. All reactions were performed in oven-dried flasks and were monitored by thin-layer chromatography (TLC) (silica gel on aluminum sheets with fluorescent dye F254, Merck KGaA). Microwave reactions were carried out using a Biotage Initiator Microwave synthesizer. NMR spectra have been recorded on a Bruker AVANCE 250 MHz, AVANCE 300 MHz or AVANCE 400 MHz instrument in deuterated solvents (euriso-top) at 25 °C. ^{1}H and ^{13}C resonances were assigned using appropriate 2D correlation spectra. Chemical shifts are reported in ppm using the solvent as internal standard. Matrix-assisted laser desorption-ionization time-of-flight (MALDI-TOF) mass spectra were obtained using an Ultraflex III TOF/TOF mass spectrometer with dithranol as matrix in reflector mode. High-resolution electrospray-ionization time-of-flight mass spectrometry (ESI-Q-TOF MS) was performed on an ESI-(Q)-TOF-MS microTOF II (Bruker Daltonics) mass spectrometer. UV−vis absorption spectra were recorded on a Perkin-Elmer Lambda 750 UV/vis spectrophotometer,

dx.doi.org/10.1021/ic402701v | Inorg. Chem. 2014, 53, 1637−1645

and emission spectra on a Jasco FP6500. Measurements were carried out using 10^{-6} M solutions of respective solvents (spectroscopy grade) in 1 cm quartz cuvettes or on dye-loaded, transparent TiO_2 anodes (12 μm thick, 0.88 cm^2 active area, see the Cell Fabrication) at room temperature. Acid−base titration was carried out in aqueous solution containing Britton−Robinson buffer (0.04 M phosphoric acid, 0.04 M acetic acid, 0.04 M boronic acid).[61] The pH value was adjusted using 2 M aqueous solutions of hydrochloric acid and sodium hydroxide. The resulting spectral behavior was monitored recording UV−vis absorption and emission spectra at distinct pH values. The variation of absorbance and emission intensity was analyzed for selected wavelengths by fitting a sigmoidal Boltzmann function to the experimental data; the obtained turning points represent the pK_a values. Emission lifetimes are mostly obtained by time-correlated single-photon counting. Here, a Titan:Sapphire laser (Tsunami, Newport Spectra-Physics GmbH) is used as the light source. The repetition rate is reduced to 400 kHz by a pulse selector (model 3980, Newport Spectra-Physics GmbH). Afterwards, the fundamental beam of the Ti-Sapphire oscillator is frequency doubled in a second harmonic generator (Newport Spectra-Physics GmbH) to create the 500-nm pump beam. The emission is detected by a Becker & Hickel PMC-100-4 photon-counting module. For these measurements the instrumental response function was on the order of several nanoseconds due to filter fluorescence. Thus, for lifetime determination the first 10−15 ns after excitation were consequently ignored. In most cases a monoexponential fitting was carried out with the rest of the data points. However, both models yield the same numerical data for the respective longer lifetime being the subject of the discussion. Since the lifetimes reported are significantly longer than the instrumental response, we claim our results with a typical uncertainty of 10%. For some measurements, excitation was carried out at 390 nm and emission was detected by a Hamamatsu HPDTA streak camera *via* a suitable spectrograph. Here, the decay curves were obtained as the spectral integral, as no spectral relaxation was observed. Samples are prepared to yield an optical density of 0.1 at the excitation wavelength. Cyclic voltammetry measurements were performed on a Metrohm Autolab PGSTAT30 potentiostat with a standard three-electrode configuration using a graphite-disk working electrode, a platinum-rod auxiliary electrode, and a Ag/AgCl reference electrode; scan rates from 50 to 500 mV·s^{-1} were applied. The experiments were carried out in degassed solvents (spectroscopy grade) containing 0.1 M Bu_4NPF_6 salt (dried previously by heating at 110 °C and storing under vacuum). At the end of each measurement, ferrocene was added as an internal standard. All calculations are based on density functional theory (DFT). The geometries of the singlet ground state and the singly oxidized ground state have been optimized for all the ruthenium(II) complexes, presented herein. The hybrid functional B3LYP[62,63] has been selected in combination with the 6-31G* basis set for all atoms. To reproduce the measured absorption UV−vis spectrum, the lowest-lying 75 vertical singlet electronic excitation energies were calculated using time-dependent DFT (TD-DFT) at the S_0 optimized geometry. The TD-DFT calculations were performed in solution using acetonitrile as solvent with the polarization continuum model and with the same functional and basis set as in the optimizations.[64,65] All these calculations were performed with the Gaussian09 program package.[66] The analysis of the EDDM calculations were performed by GaussSum2.2.[67] Electron-density difference maps (density isovalue = 0.001), Kohn−Sham orbitals (MO isovalue = 0.04), and spin-density calculations (density isovalue = 0.004) were visualized by GaussView5.0.8.[66]

Cell Fabrication. Photoanodes were prefabricated by Dyesol, Inc. (Australia) with a screen-printable TiO_2 paste (18-NRT, Dyesol). The active area of the TiO_2 electrode is 0.28 cm^2 with a thickness of 12 μm (18-NRT) and 3 μm (WER4-O) on fluorine-doped tin-oxide (FTO; TEC15 (15 Ω cm^{-2})). TiO_2 substrates were treated with $TiCl_4$(aq) (0.05 M) at 70 °C for 30 min and subsequently rinsed with H_2O and EtOH and dried prior to heating. The electrodes were heated to 450 °C for 20 min under ambient atmosphere and allowed to cool to 80 °C before dipping into the dye solution. The anode was soaked overnight for 16 h in a methanol and ethanol solution (~0.25 mM) containing the dyes **2c** and **N749**, respectively. The stained films were rinsed copiously with the solvent they were dipped in and subsequently dried. The cells were fabricated using a Pt-coated counter electrode (FTO TEC-15 (15 Ω cm^{-2})) that was heated to 450 °C for 15 min under ambient atmosphere and allowed to cool to room temperature prior to the assembling. Both electrodes were sandwiched with a 30 μm Surlyn (Dupont) gasket by resistive heating. An acetonitrile electrolyte solution, El 1 (0.6 M 1,3-dimethylimidazolium iodide (DMII), 0.06 M I_2, 0.1 M LiI, 0.5 M 4-*tert*-butylpyridine (tBP), and 0.1 M guanidinium thiocyanate (GuSCN)), El 2 (0.21 M $[Co(bpy)_3](PF_6)_2$, 0.033 M $[Co(bpy)_3](PF_6)_3$, 0.1 M $LiClO_4$, 0.5 M tBP), was introduced to the void *via* vacuum backfilling through a hole in the counter electrode. The hole was sealed with an aluminum-backed Bynel foil (Dyesol). After sealing, silver bus bars were added to all cells.[51,14]

Cell Characterization. Photovoltaic measurements were recorded with a Newport Oriel solar simulator (model 9225A1) equipped with a class A 150 W xenon light source powered by a Newport power supply (model 69907). The light output (area = 5 cm × 5 cm) was calibrated to AM 1.5 using a Newport Oriel correction filter to reduce the spectral mismatch in the region of 350−700 nm to less than 1.5%. The power output of the lamp was measured to 1 Sun (100 mW cm^{-2}) using a certified Si reference cell. The current−voltage (I−V) characteristic of each cell was obtained by applying an external potential bias to the cell and measuring the generated photocurrent with a Keithley digital source meter (model 2400). All cells were measured without a mask. IPCE measurements were performed on a QEX7 Solar Cell Spectral Response Measurement System from PV Instruments, Inc. The system was calibrated with a photodiode that was calibrated against NIST standard I755 with transfer uncertainty less than 0.5% between 400 and 1,000 nm and less than 1% at all other wavelengths. All measurements were carried out in AC mode at 4 Hz chopping frequency under a bias light between 0.01 and 0.1 sun. The system was calibrated and operated in Beam Power mode. Electrochemical impedance spectroscopy (EIS) was performed on a Gamry EIS300 potentiostat. All EIS experiments were performed in the dark and scanned the frequency range from 100 kHz to 0.5 Hz with a 10 mV voltage modulation applied to the bias.[51]

Synthesis of L1. According to the literature,[32,33] a mixture of aqueous HCHO (37%, 1.2 mL, 13.6 mmol), concentrated AcOH (96%, 0.14 mL, 2.1 mmol), and 1,4-dioxane (1.2 mL) was stirred at room temperature for 15 min. After the addition of sodium azide (153.3 mg, 2.36 mmol) and 2,6-diethynylpyridine (100 mg, 0.79 mmol), the mixture was stirred at room temperature for additional 10 min. Subsequently, concentrated aqueous solutions, first of sodium ascorbate (63 mg, 0.32 mmol) and then of $CuSO_4$ (13 mg, 0.08 mmol), were added and the resulting mixture was stirred at room temperature for 24 h. After the complete conversion of the alkyne was confirmed by TLC, EDTA was added (30 mg, 0.1 mmol), and stirring was maintained for 2h. After addition of an excess of water, the resulting suspension was filtered and washed with a minimal amount of water, and the obtained solid was kept. Additionally, the filtrate was extracted 3 times with ethyl acetate, and the organic solvent was removed *in vacuo*. The obtained solids were combined, MeOH/H_2O (1:1, 6 mL), solid NaOH (140 mg, 3.5 mmol) was added, and the mixture was stirred at room temperature for 24 h. After neutralization with 1 M HCl (3.5 mL) and addition of H_2O (30 mL), the formed precipitate was filtered, washed with water, and dried *in vacuo* to yield 128 mg (0.6 mmol, 76%) of a white solid. ^{1}H NMR (400 MHz, DMSO-d_6, ppm) δ = 15.37 (s, 2H, N*H*), 8.53 (s, 2H, N^{trz}−*H*), 8.29−7.67 (m, 3H, $H^{3a',4a',5a'}$). ^{13}C NMR (100 MHz, DMSO-d_6, ppm) δ = 149.37, 145.43, 138.27, 128.43, 118.98 MS (MALDI-TOF, dithranol): calcd for $C_{22}H_{29}N$ ($[M + H]^+$): m/z = 214.0834; found: m/z = 214.0640.

Synthesis of 2,6-Di(oct-1-yn-1-yl)pyridine. Under a nitrogen atmosphere, 2,6-dibromopyridine (2.34 g, 9.87 mmol), $Pd(PPh_3)_4$ (583 mg, 0.51 mmol, 5 mol-%), and CuI (101.2 mg, 0.53 mmol, 5 mol-%) were suspended in deaerated toluene/triethylamine (4:1, v/v 53 mL). The resulting suspension was additionally purged with nitrogen. Subsequently, 1-octyne (4.15 mL, 27.87 mmol, 2.8 equiv)

dx.doi.org/10.1021/ic402701v | *Inorg. Chem.* 2014, 53, 1637−1645

was added dropwise at room temperature to the stirred suspension. The reaction mixture was heated to 55 °C with an oil bath, and the reaction was monitored by GC-MS. After 72 h, the reaction mixture was allowed to cool to room temperature and filtered, and the remaining solid was washed with toluene. The filtrate was evaporated *in vacuo*, and the obtained solid was dissolved in CH_2Cl_2 and extracted with aqueous NH_4Cl to remove Cu(I). The organic phase was dried over Na_2SO_4, concentrated *in vacuo*, and purified by column chromatography (silica, CH_2Cl_2/*n*-hexane 1:1; R_f = 0.4). The solvents were evaporated *in vacuo* to yield 2.07 g (7.00 mmol, 71%) of a yellow oil. ^{1}H NMR (250 MHz, CD_2Cl_2, ppm) δ = 7.53 (t, ^3J = 7.8 Hz, 1H, $H^{4a\prime}$), 7.23 (d, ^3J = 7.8 Hz, 2H, $H^{3a\prime,5a\prime}$), 2.42 (t, ^3J = 7.0 Hz, 4H, CC−CH_2−CH_2−), 1.71−1.53 (m, 4H, CC−CH_2−CH_2−), 1.53−1.19 (m, 12H, −CH_2−), 0.90 (t, ^3J = 6.6 Hz, 6H, CH_3); ^{13}C NMR (63 MHz, CD_2Cl_2, ppm) δ = 144.3, 136.5, 125.7, 91.3, 80.5, 31.8, 29.1, 28.8, 22.9, 19.6, 14.2 ppm; MS (HR ESI-Q-TOF): calcd for $C_{22}H_{29}N$ ([M + H]$^+$): *m*/*z* = 296.2371; found: *m*/*z* = 296.2460.

Synthesis of PL2. A 20 mL microwave vial was charged with 2,6-di(oct-1-yn-1-yl)pyridine (1.27 g, 4.29 mmol) and azidomethyl pivalate (1.67 g, 10.65 mmol, 2.5 equiv). The vial was capped and heated to 100 °C in an oil bath for 72 h. The completion of the reaction was confirmed by TLC (alumina, CH_2Cl_2) and GC-MS. All volatiles were removed *in vacuo*, and the remaining solid was subjected to column chromatography (alumina, CH_2Cl_2/*n*-hexane, 3:1). All product fractions (irrespective of the regioisomer) were combined to yield 1.99 g (3.27 mmol, 76%) of a brown oil. For the NMR analysis, the asymmetric product (see Scheme 1) was used exemplarily. ^{1}H NMR (250 MHz, CD_2Cl_2, ppm) δ = 8.28 (d, ^3J = 8.0 Hz, 1H, $H^{3a\prime}$), 7.94 (t, ^3J = 7.9 Hz, 1H, $H^{4a\prime}$), 7.38 (d, ^3J = 7.6 Hz, 1H, $H^{5a\prime}$), 6.44 (s, 2H, N−CH_2−O), 6.27 (s, 2H, N^{trz}−CH_2−O), 3.33−2.99 (m, 2H, C^{5a}−CH_2−CH_2), 2.88−2.67 (m, 2H, C$^{5a\prime\prime}$−CH_2−CH_2), 1.79−1.45 (m, 4H, C$^{5a,5a\prime\prime}$−CH_2−CH_2), 1.35−1.07 (m, 21H, CH_2, $H^{tert\text{-}butyl}$), 0.96 (s, 9H, −CH_3), 0.92−0.59 (m, 6H, $H^{tert\text{-}butyl}$); ^{13}C NMR (63 MHz, CD_2Cl_2, ppm) δ = 177.1, 176.7, 152.9, 147.2, 147.1, 143.0, 138.4, 138.0, 133.5, 123.4, 121.5, 70.3, 69.1, 39.1, 38.9, 31.8, 31.7, 29.6, 29.4, 29.2, 29.2, 27.0, 26.8, 25.5, 23.5, 22.9, 22.8, 14.2, 14.1; MS (HR ESI-Q-TOF): calcd for $C_{33}H_{52}N_7O_4$ ([M + H]$^+$): *m*/*z* = 610.4081; found: *m*/*z* = 610.4084.

Synthesis of L2. According to the literature,[33] **PL2** (1.4 g, 2.29 mmol) and NaOH (210 mg, 5.25 mmol, 4.4 equiv) were dissolved in MeOH/H_2O (1:1, *v*/*v* 30 mL) and the mixture was stirred at room temperature. The full conversion of the educt was determined by TLC (alumina, CH_2Cl_2). After 24 h, the reaction mixture was dropped into HCl_{aq} (0.175 M) and, subsequently, neutralized with $NaHCO_3$. The precipitated product was filtered, washed with water, and dried *in vacuo* to yield 650 mg (1.71 mmol, 74%) of a colorless solid. ^{1}H NMR (250 MHz, DMSO-d_6, ppm) δ = 15.20 (s, 1H, N−*H*), 14.80 (s, 1H, N−*H*), 7.93 (m, 3H, $H^{3a\prime,4a\prime,5a\prime}$), 3.26−2.88 (m, 4H, C$^{5a,5a\prime\prime}$−$CH_2$−), 1.80−1.43 (m, 4H, C$^{5a,5a\prime\prime}$−$CH_2$−$CH_2$−), 1.38−1.04 (m, 12H, −$CH_2$−), 0.85−0.63 (m, 6H, −$CH_3$). ^{13}C NMR (63 MHz, DMSO-d_6, ppm) δ = 151.6, 151.1, 145.2, 142.7, 141.1, 137.6, 135.9, 120.4, 112.0, 119.7, 119.3, 31.0, 30.9, 28.2, 25.2, 22.8, 21.9, 13.8; MS (HR ESI-Q-TOF): calcd for $C_{21}H_{31}N_7Na$ ([M + Na]$^+$): *m*/*z* = 404.2538; found: *m*/*z* = 404.2513. Elem. anal. calcd for $C_{21}H_{31}N_7$ (381.52): C, 66.11%; H, 8.19%; N, 25.70%; found: C, 64.93%; H, 8.78%, N, 25.82%.

Synthesis of 1. A 10 mL microwave vial was charged with **L1** (50 mg, 0.23 mmol), [Ru(tpy)(MeCN)$_3$](PF$_6$)$_2$ (175 mg, 0.23 mmol), and EtOH (8 mL). The vial was capped and the suspension was purged with nitrogen for 10 min. Subsequently, the mixture was heated to 150 °C for 30 min in the microwave reactor. NEt_3 (1 mL) was added to the reaction mixture to complete the precipitation. The dark precipitate was filtered and washed thoroughly with MeOH/NEt_3 (9:1, *v*/*v*) and, subsequently, with CH_2Cl_2. The obtained solid was allowed to dry upon standing, yielding 99 mg (0.18 mmol, 77%) of a dark brown solid. Due to the low solubility of the charge-neutral complex, some drops of trifluoroacetic acid (TFA) were added for the NMR analysis. A ^{13}C NMR spectrum could not be recorded, owing to the low solubility. ^{1}H NMR (400 MHz, CD_2Cl_2 + CF_3COOH, ppm) δ = 8.68 (s, 2H, $H^{5a,5a\prime\prime}$), 8.48 (d, ^3J = 8.1, 2H, $H^{3\prime,5\prime}$), 8.40−8.21 (m, 6H, $H^{3a\prime,4a\prime,5a\prime,\ 4\prime,\ 3,3\prime\prime}$), 7.91 (td, ^3J = 7.9 Hz, ^4J = 1.5 Hz, 2H, $H^{4,4\prime\prime}$), 7.29 (d, ^3J = 4.9 Hz, 2H, $H^{6,6\prime\prime}$), 7.18 (ddd, ^3J = 7.5, 5.5 Hz, ^4J = 1.2 Hz, 2H, $H^{5,5\prime\prime}$); MS (MALDI-TOF, dithranol): calcd for $C_{36}H_{41}N_{10}Ru$ ([M + H]$^+$): *m*/*z* = 547.0691; found: *m*/*z* = 547.0840.

Note: Under the reaction conditions, a partial triazole *N*-alkylation,[68] presumably due to the formation of a carbenium ion from the alcohol solvent under the acidic reaction conditions was observed; however, the minor side product was easily removed by trituration of the reaction mixture with MeOH/NEt_3 (9:1, *v*/*v*). Nonetheless, TEGDME was chosen as solvent in case of **2b** (*vide infra*) in order to circumvent this side reaction.

Synthesis of 2a. A 20 mL microwave vial was charged with **L2** (160 mg, 0.419 mmol), [Ru(tpy)(MeCN)$_3$](PF$_6$)$_2$ (313 mg, 0.419 mmol), and EtOH (17 mL). The vial was capped and the suspension purged with nitrogen for 10 min. Subsequently, the mixture was heated to 160 °C for 30 min in the microwave reactor. The full conversion of the precursor was proven by TLC (silica, MeCN/H_2O/aq KNO_3 40:4:1). NEt_3 was added to the crude product mixture to ensure complete deprotonation. Afterwards, the black solid was filtered and thoroughly washed with EtOH/NEt_3 (9:1, *v*/*v*). The solid was dried and suspended in MeOH/NEt_3 (9:1, *v*/*v*), filtered, washed again with MeOH/NEt_3 (9:1, *v*/*v*), and dried to yield 215 mg (0.301 mmol, 72%) of a black solid. Due to the low solubility of the charge-neutral complex, TFA was added for NMR analysis. ^{1}H NMR (400 MHz, CD_2Cl_2 + CF_3COOH, ppm) δ = 8.45 (d, ^3J = 8.1 Hz, 2H, $H^{3\prime,5\prime}$), 8.32−8.19 (m, 4H, $H^{3,3\prime\prime,4\prime,4a\prime}$), 8.04 (d, ^3J = 8.1 Hz, 2H, $H^{3a\prime,5a\prime}$), 7.87 (t, ^3J = 7.8 Hz, 2H, $H^{4,4\prime\prime}$), 7.26 (d, ^3J = 5.1 Hz, 2H, $H^{6,\ 6\prime\prime}$), 7.15 (d, ^3J = 6.4 Hz, 2H, $H^{5,\ 5\prime\prime}$), 3.23−3.04 (m, 4H, C$^{5a,5a\prime\prime}$−CH_2−), 1.86−1.64 (m, 4H, C$^{5a,5a\prime\prime}$−CH_2−CH_2−), 1.48−1.17 (m, 12H, −CH_2−), 1.04−0.77 (m, 6H, −CH_3); ^{13}C NMR (100 MHz, CD_2Cl_2 + CF_3COOH, ppm) δ = 159.0, 156.7, 152.0, 151.2, 144.1, 141.1, 138.1, 137.1, 135.8, 127.6, 124.1, 122.7, 118.6, 31.5, 29.1, 28.6, 24.0, 22.8, 14.0; MS (HR ESI-Q-TOF): calcd for $C_{36}H_{41}N_{10}Ru$ ([M + H]$^+$): *m*/*z* = 715.2550; found: *m*/*z* = 715.2328.

Synthesis of 2b. A 10 mL microwave vial was loaded with [Ru(tcmtpy)(MeCN)$_3$](PF$_6$)$_2$ (80 mg, 0.086 mmol), **L2** (33 mg, 0.086 mmol), and TEGDME (4.8 mL) The vial was capped, and the solution was purged with nitrogen for 10 min. Subsequently, the reaction mixture was heated to 150 °C for 30 min in the microwave reactor. After the full conversion of [Ru(tcmtpy)(MeCN)$_3$](PF$_6$)$_2$ was confirmed by TLC (silica, MeCN/H_2O/aq KNO_3 40:4:1), the reaction mixture was dropped into H_2O and the precipitate was filtered, washed with H_2O, rinsed with MeCN, and subjected to column chromatography (silica, MeCN/MeOH 9:1). Subsequently, the product was precipitated in H_2O from a concentrated MeCN solution, additionally washed with H_2O, and rinsed with MeCN. After evaporation of the solvent *in vacuo*, 44 mg (0.049 mmol, 58%) of a red solid were obtained. ^{1}H NMR (400 MHz, CD_2Cl_2, ppm) δ = 9.08 (s, 2H, $H^{3\prime,5\prime}$), 8.85 (s, 2H, $H^{3,3\prime\prime}$), 8.04 (t, *J* = 7.9 Hz, 1H, $H^{4a\prime}$), 7.71 (d, *J* = 8.0 Hz, 2H, $H^{3a\prime,5a\prime}$), 7.62 (d, *J* = 4.3 Hz, 2H, $H^{5,5\prime\prime}$), 7.58 (d, *J* = 5.8 Hz, 2H, $H^{6,6\prime\prime}$), 4.16 (s, 3H, −COOCH_3′), 3.95 (s, 6H, −COOCH_3), 2.94 (t, 4H, C$^{5a,5a\prime\prime}$−CH_2−), 1.75−1.62 (m, 4H, C$^{5a,5a\prime\prime}$−CH_2−CH_2−), 1.34 (m, 12H, −CH_2−), 0.87 (d, *J* = 6.5 Hz, 6H, −CH_3); ^{13}C NMR (100 MHz, CD_2Cl_2, ppm) δ = 165.1, 164.2, 159.6, 157.3, 152.4, 152.0, 146.8, 141.0, 137.2, 136.8, 132.4, 126.3, 122.2, 121.5, 114.7, 53.5, 53.4, 32.0, 29.8, 29.6, 26.9, 23.0, 14.2; MS (HR ESI-Q-TOF): calcd for $C_{42}H_{47}N_{10}O_6Ru$ ([M + H]$^+$): *m*/*z* = 889.2730; found: *m*/*z* = 889.2861.

Synthesis of 2c. According to the literature,[12,69] **2b** (30 mg, 0.03 mmol) was suspended in DMF/NEt_3/H_2O (3:1:1, *v*/*v* 3 mL) and heated to reflux under a nitrogen atmosphere. After 36 h, the full conversion was confirmed with MS (MALDI ToF) and the solvents were evaporated *in vacuo*. The resultant solid was suspended in CH_2Cl_2 and collected by centrifugation. The solvent was decanted, and this procedure was repeated twice with CH_2Cl_2 and once with MeOH. The remaining solid was dried *in vacuo* to obtain 16 mg (0.02 mmol, 56%) of a brown solid. ^{1}H NMR (400 MHz, MeOD, ppm) δ = 9.23 (s, 2H, $H^{3\prime,5\prime}$), 9.02 (s, 2H, $H^{3,3\prime\prime}$), 8.36 (t, *J* = 7.9 Hz, 1H, $H^{4a\prime}$), 8.22 (d, *J* = 8.1 Hz, 2H, $H^{3a\prime,5a\prime}$), 7.70 (d, *J* = 5.7 Hz, 2H, $H^{5,5\prime\prime}$), 7.58 (d, *J* = 5.5 Hz, 2H, $H^{6,6\prime\prime}$), 3.19−3.10 (m, 4H, C$^{5a,5a\prime\prime}$−CH_2−), 1.84−

dx.doi.org/10.1021/ic402701v | *Inorg. Chem.* 2014, 53, 1637−1645

1.72 (m, 4H, $C^{5a,5a''}-CH_2-CH_2-$), 1.48−1.25 (m, 12H, $-CH_2-$), 0.88 (t, J = 7.0 Hz, 6H, $-CH_3$); MS (MALDI-TOF, dithranol): calcd for $C_{39}H_{40}N_{10}O_6Ru$ ($[M + H]^+$): m/z = 847.2780; found: m/z = 847.2221.

■ ASSOCIATED CONTENT

Supporting Information

Additional computational, photophysical, electrochemical, and EIS data as well as NMR and MS spectra. This material is available free of charge *via* the Internet at http://pubs.acs.org.

■ AUTHOR INFORMATION

Corresponding Author

*E-mail: benjamin.dietzek@uni-jena.de (B.D.), cberling@chem.ubc.ca (C.P.B.), ulrich.schubert@uni-jena.de (U.S.S.).

Author Contributions

△S.S. and B.S. contributed equally to this work.

Notes

The authors declare no competing financial interests.

■ ACKNOWLEDGMENTS

B.S. and C.F. are grateful to the Fonds der Chemischen Industrie for Ph.D. scholarships. B.D. thanks the Fonds der Chemischen Industrie for financial support. M.J. is grateful to the Carl Zeiss foundation for financial support. D.G.B. and C.P.B. are grateful to the Canadian Natural Science and Engineering Research Council, the Canadian Foundation for Innovation, Alberta Ingenuity, and the Alfred P. Sloan Foundation for support.

■ REFERENCES

(1) O'Regan, B.; Grätzel, M. *Nature* **1991**, *353*, 737.

(2) Hagfeldt, A.; Boschloo, G.; Sun, L.; Kloo, L.; Pettersson, H. *Chem. Rev.* **2010**, *110*, 6595.

(3) Yella, A.; Lee, H.-W.; Tsao, H. N.; Yi, C.; Chandiran, A. K.; Nazeeruddin, M. K.; Diau, E. W.-G.; Yeh, C.-Y.; Zakeeruddin, S. M.; Grätzel, M. *Science* **2011**, *334*, 629.

(4) Nazeeruddin, M. K.; Péchy, P.; Renouard, T.; Zakeeruddin, S. M.; Humphry-Baker, R.; Comte, P.; Liska, P.; Cevey, L.; Costa, E.; Shklover, V.; Spiccia, L.; Deacon, G. B.; Bignozzi, C. A.; Grätzel, M. *J. Am. Chem. Soc.* **2001**, *123*, 1613.

(5) Chiba, Y.; Islam, A.; Watanabe, Y.; Komiya, R.; Koide, N.; Han, L. *Jpn. J. Appl. Phys.* **2006**, *45*, L638.

(6) Reynal, A.; Palomares, E. *Eur. J. Inorg. Chem.* **2011**, 4509.

(7) Han, L.; Islam, A.; Chen, H.; Malapaka, C.; Chiranjeevi, B.; Zhang, S.; Yang, X.; Yanagida, M. *Energy Environ. Sci.* **2012**, *5*, 6057.

(8) Nour-Mohhamadi, F.; Nguyen, S. D.; Boschloo, G.; Hagfeldt, A.; Lund, T. *J. Phys. Chem. B* **2005**, *109*, 22413.

(9) Nguyen, P. T.; Degn, R.; Nguyen, H. T.; Lund, T. *Sol. Energy Mater. Sol. Cells* **2009**, *93*, 1939.

(10) Bessho, T.; Yoneda, E.; Yum, J.-H.; Guglielmi, M.; Tavernelli, I.; Imai, H.; Rothlisberger, U.; Nazeeruddin, M. K.; Grätzel, M. *J. Am. Chem. Soc.* **2009**, *131*, 5930.

(11) Wadman, S. H.; Kroon, J. M.; Bakker, K.; Lutz, M.; Spek, A. L.; van Klink, G. P. M.; van Koten, G. *Chem. Commun.* **2007**, 1907.

(12) Robson, K. C. D.; Koivisto, B. D.; Yella, A.; Sporinova, B.; Nazeeruddin, M. K.; Baumgartner, T.; Grätzel, M.; Berlinguette, C. P. *Inorg. Chem.* **2011**, *50*, 5494.

(13) Pogozhev, D. V.; Bezdek, M. J.; Schauer, P. A.; Berlinguette, C. P. *Inorg. Chem.* **2013**, *52*, 3001.

(14) Bomben, P. G.; Gordon, T. J.; Schott, E.; Berlinguette, C. P. *Angew. Chem., Int. Ed.* **2011**, *50*, 10682.

(15) Kisserwan, H.; Ghaddar, T. H. *Dalton Trans.* **2011**, *40*, 3877.

(16) Schulze, B.; Brown, D. G.; Robson, K. C. D.; Friebe, C.; Jäger, M.; Birckner, E.; Berlinguette, C. P.; Schubert, U. S. *Chem.—Eur. J.* **2013**, *19*, 14171.

(17) Dragonetti, C.; Colombo, A.; Magni, M.; Mussini, P.; Nisic, F.; Roberto, D.; Ugo, R.; Valore, A.; Valsecchi, A.; Salvatori, P.; Lobello, M. G.; De Angelis, F. *Inorg. Chem.* **2013**, *52*, 10723.

(18) Hsu, C.-W.; Ho, S.-T.; Wu, K.-L.; Chi, Y.; Liu, S.-H.; Chou, P.-T. *Energy Environ. Sci.* **2012**, *5*, 7549.

(19) Yeh, H.-H.; Ho, S.-T.; Chi, Y.; Clifford, J. N.; Palomares, E.; Liu, S.-H.; Chou, P.-T. *J. Mater. Chem. A* **2013**, *1*, 7681.

(20) Wang, S.-W.; Wu, K.-L.; Ghadiri, E.; Lobello, M. G.; Ho, S.-T.; Chi, Y.; Moser, J.-E.; De Angelis, F.; Grätzel, M.; Nazeeruddin, M. K. *Chem. Sci.* **2013**, *4*, 2423.

(21) Wu, K.-L.; Li, C.-H.; Chi, Y.; Clifford, J. N.; Cabau, L.; Palomares, E.; Cheng, Y.-M.; Pan, H.-A.; Chou, P.-T. *J. Am. Chem. Soc.* **2012**, *134*, 7488.

(22) Wu, K.-L.; Hsu, H.-C.; Chen, K.; Chi, Y.; Chung, M.-W.; Liu, W.-H.; Chou, P.-T. *Chem. Commun.* **2010**, *46*, 5124.

(23) Chou, C.-C.; Wu, K.-L.; Chi, Y.; Hu, W.-P.; Yu, S. J.; Lee, G.-H.; Lin, C.-L.; Chou, P.-T. *Angew. Chem., Int. Ed.* **2011**, *50*, 2054.

(24) Bomben, P. G.; Robson, K. C. D.; Koivisto, B. D.; Berlinguette, C. P. *Coord. Chem. Rev.* **2012**, *256*, 1438.

(25) Wang, M.; Moon, S.-J.; Zhou, D.; Le Formal, F.; Cevey-Ha, N.-L.; Humphry-Baker, R.; Grätzel, C.; Wang, P.; Zakeeruddin, S. M.; Grätzel, M. *Adv. Funct. Mater.* **2010**, *20*, 1821.

(26) Wang, P.; Zakeeruddin, S. M.; Moser, J. E.; Nazeeruddin, M. K.; Sekiguchi, T.; Grätzel, M. *Nat. Mater.* **2003**, *2*, 402.

(27) Zakeeruddin, S. M.; Nazeeruddin, M. K.; Humphry-Baker, R.; Péchy, P.; Quagliotto, P.; Barolo, C.; Viscardi, G.; Grätzel, M. *Langmuir* **2002**, *18*, 952.

(28) Crowley, J. D.; McMorran, D. A. In *Topics in Heterocyclic Chemistry: Click Triazoles*; Košmrlj, J., Ed.; Springer: Berlin Heidelberg, 2012; Vol. *28*, p 31.

(29) Struthers, H.; Mindt, T. L.; Schibli, R. *Dalton Trans.* **2010**, *39*, 675.

(30) Schulze, B.; Schubert, U. S. *Chem. Soc. Rev.*, in press, DOI: 10.1039/c3cs60386e.

(31) Duati, M.; Tasca, S.; Lynch, F. C.; Bohlen, H.; Vos, J. G.; Stagni, S.; Ward, M. D. *Inorg. Chem.* **2003**, *42*, 8377.

(32) Kalisiak, J.; Sharpless, K. B.; Fokin, V. V. *Org. Lett.* **2008**, *10*, 3171.

(33) Loren, J. C.; Krasiński, A.; Fokin, V. V.; Sharpless, K. B. *Synlett* **2005**, 2847.

(34) Schulze, B.; Escudero, D.; Friebe, C.; Siebert, R.; Görls, H.; Sinn, S.; Thomas, M.; Mai, S.; Popp, J.; Dietzek, B.; González, L.; Schubert, U. S. *Chem.—Eur. J.* **2012**, *18*, 4010.

(35) Nazeeruddin, M. K.; Humphry-Baker, R.; Liska, P.; Grätzel, M. *J. Phys. Chem. B* **2003**, *107*, 8981.

(36) Benkö, G.; Kallioinen, J.; Myllyperkiö, P.; Trif, F.; Korppi-Tommola, J. E. I.; Yartsev, A. P.; Sundström, V. *J. Phys. Chem. B* **2004**, *108*, 2862.

(37) Clifford, J. N.; Palomares, E.; Nazeeruddin, M. K.; Grätzel, M.; Durrant, J. R. *J. Phys. Chem. C* **2007**, *111*, 6561.

(38) Jeon, J.; Goddard, W. A., III; Kim, H. *J. Am. Chem. Soc.* **2013**, *135*, 2431.

(39) Schulze, B.; Friebe, C.; Hager, M. D.; Winter, A.; Hoogenboom, R.; Görls, H.; Schubert, U. S. *Dalton Trans.* **2009**, 787.

(40) Duati, M.; Fanni, S.; Vos, J. G. *Inorg. Chem. Commun.* **2000**, *3*, 68.

(41) Buchanan, B. E.; Vos, J. G.; Kaneko, M.; van der Putten, W. J. M.; Kelly, J. M.; Hage, R.; de Graaff, R. A. G.; Prins, R.; Haasnoot, J. G.; Reedijk, J. *J. Chem. Soc., Dalton Trans.* **1990**, 2425.

(42) Amini, A.; Harriman, A.; Mayeux, A. *Phys. Chem. Chem. Phys.* **2004**, *6*, 1157.

(43) Listorti, A.; O'Regan, B.; Durrant, J. R. *Chem. Mater.* **2011**, *23*, 3381.

(44) Katritzky, A. R.; Ramsden, C. A.; Joule, J. A.; Zhdankin, V. V. In *Handbook of Heterocyclic Chemistry*, 3rd ed; Elsevier: Amsterdam, 2010; p 473.

(45) Lancaster, K. M.; Gerken, J. B.; Durrell, A. C.; Palmer, J. H.; Gray, H. B. *Coord. Chem. Rev.* **2010**, *254*, 1803.

(46) Thompson, D. W.; Ito, A.; Meyer, T. J. *Pure Appl. Chem.* **2013**, *85*, 1257.
(47) Boschloo, G.; Gibson, E. A.; Hagfeldt, A. *J. Phys. Chem. Lett.* **2011**, *2*, 3016.
(48) Abrahamsson, M.; Jäger, M.; Österman, T.; Eriksson, L.; Persson, P.; Becker, H.-C.; Johansson, O.; Hammarström, L. *J. Am. Chem. Soc.* **2006**, *128*, 12616.
(49) Pavlishchuk, V. V.; Addison, A. W. *Inorg. Chim. Acta* **2000**, *298*, 97.
(50) Connelly, N. G.; Geiger, W. E. *Chem. Rev.* **1996**, *96*, 877.
(51) Bomben, P. G.; Borau-Garcia, J.; Berlinguette, C. P. *Chem. Commun.* **2012**, *48*, 5599.
(52) Lee, K.-M.; Suryanarayanan, V.; Ho, K.-C.; Justin Thomas, K. R.; Lin, J. T. *Sol. Energy Mater. Sol. Cells* **2007**, *91*, 1426.
(53) Fabregat-Santiago, F.; Bisquert, J.; Garcia-Belmonte, G.; Boschloo, G.; Hagfeldt, A. *Sol. Energy Mater. Sol. Cells* **2005**, *87*, 117.
(54) Bisquert, J. *Phys. Chem. Chem. Phys.* **2003**, *5*, 5360.
(55) Bisquert, J.; Fabregat-Santiago, F. In *Dye-sensitized Solar Cells*, 1st ed.; Kalyanasundaram, K., Ed.; EPFL Press: Lausanne, 2010; p 457.
(56) Fabregat-Santiago, F.; Garcia-Belmonte, G.; Mora-Seró, I.; Bisquert, J. *Phys. Chem. Chem. Phys.* **2011**, *13*, 9083.
(57) Yu, Z.; Vlachopoulos, N.; Gorlov, M.; Kloo, L. *Dalton Trans.* **2011**, *40*, 10289.
(58) Hamann, T. W. *Dalton Trans.* **2012**, *41*, 3111.
(59) Klahr, B. M.; Hamann, T. W. *J. Phys. Chem. C* **2009**, *113*, 14040.
(60) Shin, Y.; Fryxell, G. E.; Johnson, C. A., II; Haley, M. M. *Chem. Mater.* **2008**, *20*, 981.
(61) Britton, H. T. S.; Robinson, R. A. *J. Chem. Soc.* **1931**, 1456.
(62) Becke, A. D. *J. Chem. Phys.* **1993**, *98*, 5648.
(63) Lee, C.; Yang, W.; Parr, R. G. *Phys. Rev. B* **1988**, *37*, 785.
(64) Mennucci, B.; Tomasi, J. *J. Chem. Phys.* **1997**, *106*, 5151.
(65) Cossi, M.; Barone, V.; Mennucci, B.; Tomasi, J. *Chem. Phys. Lett.* **1998**, *286*, 253.
(66) Frisch, M. J.; Trucks, G. W.; Schlegel, H. B.; Scuseria, G. E.; Robb, M. A.; Cheeseman, J. R.; Scalmani, G.; Barone, V.; Mennucci, B.; Petersson, G. A.; Nakatsuji, H.; Caricato, M.; Li, X.; Hratchian, H. P.; Izmaylov, A. F.; Bloino, J.; Zheng, G.; Sonnenberg, J. L.; Hada, M.; Ehara, M.; Toyota, K.; Fukuda, R.; Hasegawa, J.; Ishida, M.; Nakajima, T.; Honda, Y.; Kitao, O.; Nakai, H.; Vreven, T.; Montgomery, J. A.; Peralta, J. E.; Ogliaro, F.; Bearpark, M.; Heyd, J. J.; Brothers, E.; Kudin, K. N.; Staroverov, V. N.; Kobayashi, R.; Normand, J.; Raghavachari, K.; Rendell, A.; Burant, J. C.; Iyengar, S. S.; Tomasi, J.; Cossi, M.; Rega, N.; Millam, J. M.; Klene, M.; Knox, J. E.; Cross, J. B.; Bakken, V.; Adamo, C.; Jaramillo, J.; Gomperts, R.; Stratmann, R. E.; Yazyev, O.; Austin, A. J.; Cammi, R.; Pomelli, C.; Ochterski, J. W.; Martin, R. L.; Morokuma, K.; Zakrzewski, V. G.; Voth, G. A.; Salvador, P.; Dannenberg, J. J.; Dapprich, S.; Daniels, A. D.; Farkas; Foresman, J. B.; Ortiz, J. V.; Cioslowski, J.; Fox, D. J., *Gaussian 09*, Revision B.01; Gaussian Inc.: Wallingford, CT, 2009.
(67) O'Boyle, N. M.; Tenderholt, A. L.; Langner, K. M. *J. Comput. Chem.* **2008**, *29*, 839.
(68) Timokhin, B. V.; Golubin, A. I.; Vysotskaya, O. V.; Kron, V. A.; Oparina, L. A.; Gusarova, N. K.; Trofimov, B. A. *Chem. Heterocycl. Compd.* **2002**, *38*, 981.
(69) Bomben, P. G.; Thériault, K. D.; Berlinguette, C. P. *Eur. J. Inorg. Chem.* **2011**, 1806.